Nonequilibrium interactions between ideal polymers and a repulsive surface

Raz Halifa Levi* and Yacov Kantor
Raymond and Beverly Sackler School of Physics and Astronomy, Tel Aviv University, Tel Aviv 69978, Israel
(Received 25 April 2017; published 23 August 2017)

We use Newtonian and overdamped Langevin dynamics to study long flexible polymers dragged by an external force at a constant velocity v. The work W performed by that force depends on the initial state of the polymer and the details of the process. The Jarzynski equality can be used to relate the nonequilibrium work distribution $P(W)$ obtained from repeated experiments to the equilibrium free energy difference ΔF between the initial and final states. We use the power law dependence of the geometrical and dynamical characteristics of the polymer on the number of monomers N to suggest the existence of a critical velocity $v_c(N)$, such that for $v < v_c$ the reconstruction of ΔF is an easy task, while for v significantly exceeding v_c it becomes practically impossible. We demonstrate the existence of such v_c analytically for an ideal polymer in free space and numerically for a polymer which is being dragged away from a repulsive wall. Our results suggest that the distribution of the dissipated work $W_{\rm d} = W - \Delta F$ in properly scaled variables approaches a limiting shape for large N.

DOI: 10.1103/PhysRevE.96.022146

I. INTRODUCTION

Equilibrium interactions between a single polymer and a repulsive surface have been a subject of intensive study for several decades [1–3] and benefited from the relation between the statistical mechanics of polymers and the general theory of phase transitions [4–7]. Current experimental methods allow a detailed study of biological macromolecules [8,9]. In particular, atomic force microscopy [10–12] is an important tool in measuring force-displacement curves of biomolecules, and reconstruction of their free energy and spatial structure [13].

A long polymer held by its end at a distance h from a repulsive flat surface (wall) experiences an *equilibrium repulsive* force $f_{\rm eq}(h)$, i.e., to keep the polymer in place an external force $f = -f_{\rm eq}$ towards the wall must be applied at the end of the polymer. If h is significantly larger than the microscopic length scale a, such as monomer size or persistence length, but is much smaller than the root-mean-square (rms) end-to-end distance R of the polymer, then the expression for the force, at temperature T, has a particularly simple form,

$$f_{\rm eq}(h) = \mathcal{A}\frac{k_{\rm B}T}{h}, \tag{1}$$

where the dimensionless prefactor $\mathcal{A}$ can be related to the critical exponents of the polymer [14,15]. (For nonflat scale-free repulsive surfaces, such as cones, the prefactor $\mathcal{A}$ depends on the surface geometry [14–17]). In many cases the polymer size R is related to the number of monomers N by $R \approx aN^{\nu}$. In particular, for an *ideal* polymer, in which the interactions between nonadjacent monomers are neglected, $\nu = \frac{1}{2}$, while for polymers in good solvents $\nu \approx 0.59$ [2]. Thus, the work W performed by an external agent while moving a polymer *slowly* away from a surface at fixed T, as well as the free energy difference $\Delta F = F_{\rm f} - F_{\rm i}$, between the final free energy of the polymer in free space $F_{\rm f}$ and the initial free energy when the polymer is attached to the surface $F_{\rm i}$, is

$$W = \Delta F = \int_0^{\infty} f(h)dh \approx -\int_a^R f_{\rm eq}(h)dh = -\mathcal{A}\nu k_{\rm B}T \ln N. \tag{2}$$

For an ideal polymer near a flat surface $\mathcal{A}\nu = \frac{1}{2}$ [14,15]. The negative sign reflects the need to push the polymer *towards* the wall as we *slowly* move it away.

Equation (1) for the force and the resulting Eq. (2) correspond to quasistatic motions. However, if the change is performed at a finite rate, then the work W of the external agent will depend on the details of the experimental protocol, as well as on the microscopic initial state of the system and the specific realization of thermal noise, if such is present. Consider a situation where the initial state, such as a polymer attached to the wall, corresponds to an equilibrium situation at temperature T, i.e., is selected from a canonical ensemble. When an external agent follows an experimental protocol and performs work W, the system reaches a new nonequilibrium state, such as having a polymer far away from a wall. If we proceed to equilibrate the system at temperature T, it settles into a state characterized by the free energy $F_{\rm f}$. Repeated nonequilibrium experiments result in the work distribution $P(W)$. A remarkable relation derived by Jarzynski [18,19] relates the *exact* distribution $P(W)$ to the change of the free energy ΔF between the final equilibrated state and the initial equilibrium state by

$$\langle e^{-\beta W}\rangle = \int_{-\infty}^{\infty} e^{-\beta W}P(W){\rm d}W = e^{-\beta\Delta F}, \tag{3}$$

where $\beta = 1/k_BT$ and $\langle\cdot\rangle$ denotes averaging over the initial states and over realizations of thermal noise, if such is present.

At first sight, the Jarzynski equality (JE) provides a tool for easy calculation of free energies from nonequilibrium measurements, and it has been used to reconstruct free energies in certain situations [20–23]. However, it has been observed that for a system significantly out of equilibrium, the successful use of Eq. (3) requires an accurate knowledge of the probabilities of nontypical (rare) events [24]. (This can be explicitly observed in the rare cases of exactly solvable systems, such as a

*razhalifa@gmail.com

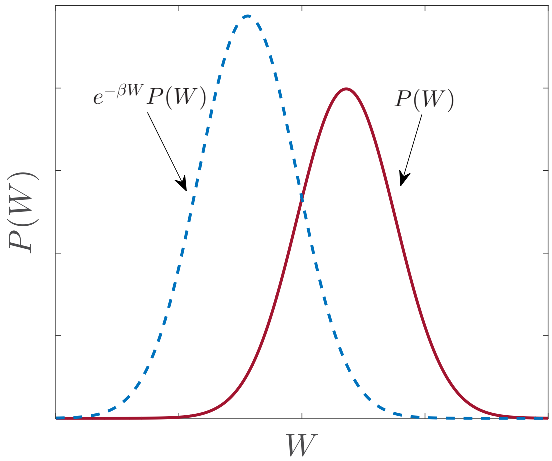

FIG. 1. Illustration of the distribution of work $P(W)$ (solid line) and the shifted function $G = e^{-\beta W}P(W)$ (dashed line). P is measured by repeating the experiment, and G needs to be reconstructed from the approximate knowledge of P.

one-dimensional Jepsen gas [25,26].) From the mathematical point of view, this happens when the integrand of Eq. (3) $G(W) \equiv e^{-\beta W}P(W)$ has a peak centered well below the position of the peak of $P(W)$, i.e., the distance between the peaks exceeds the width of $P(W)$, as illustrated in Fig. 1. In the latter situation, the function $G(W)$ is reconstructed from the *tail* of $P(W)$, which cannot be accurately estimated with a moderate number of repeated experiments. The separation of G and P increases with departure from equilibrium in the experiment. A convenient measure of this departure is the mean of the *dissipated work* $W_{\rm d} \equiv W - \Delta F$. This $\langle W_{\rm d}\rangle$ vanishes in quasistatic isothermal processes and increases with increasing rate of the processes, and when it exceeds several k_BT the free energy reconstruction becomes unreliable. (It has been shown that the number of repeated experiments required for a reliable reconstruction of ΔF increases exponentially with $\langle W_{\rm d}\rangle$ of a *reverse* process [27].) Thus, the borderline between easy measurements and practically impossible ones is rather abrupt.

In this paper we consider the problem of a polymer, which is initially in equilibrium near a flat repulsive wall, and is being dragged away with a constant velocity v. The final state is when the polymer is in equilibrium far away from the wall, such that we can treat it as being in free space. The dynamics of the system will be either overdamped Langevin dynamics, in which the inertia term is neglected, or Newtonian dynamics in which friction and thermal noise are absent. We argue that there is a critical pulling velocity v_c, such that for $v < v_c$ reconstruction of ΔF is possible by using JE, while for $v > v_c$ such reconstruction is practically impossible. In our discussion we will focus only on these two extreme cases, and we will not consider the range of velocities around v_c for which the ability of reconstruction strongly depends on the number of experiments. In Sec. II we present a heuristic argument for calculating v_c in rather general circumstances. In the remainder of the paper, we provide supporting evidence for the analytically solvable case of ideal polymers in free space (Sec. III) and for the numerically solved case of an ideal polymer near a flat repulsive surface (Sec. IV). In Sec. V we summarize our results, and discuss their possible generalizations. Since our work relies on the known results of a dragged harmonic oscillator, we provide a short summary of these properties in Appendix.

II. CRITICAL DRAGGING VELOCITY: A HEURISTIC ARGUMENT

Consider a situation in which a large polymer is being dragged away from a repulsive wall by moving its end monomer at a constant velocity v. In the initial (equilibrium) state the end monomer is attached to the wall, and in the final state the end monomer is at a distance significantly exceeding the polymer size R, so that interactions with the wall can be ignored.

Many equilibrium properties of polymers have a simple power-law dependence on the number of monomers N. In many cases dynamic features also have that property [4,6,7]. We would like to take advantage of these scaling properties of polymers to estimate the critical velocity v_c, which defines the borderline between "fast" and "slow" dragging.

Let us first consider the simple case of a polymer prepared in thermal equilibrium, and subsequently disconnected from the thermal bath, i.e., its subsequent motion will be determined by *Newtonian dynamics* (ND). For a polymer at equilibrium, the velocity of its center of mass is $\mathbf{v}_{\rm cm} = \frac{1}{N}\sum_{i=1}^{N}\mathbf{v}_i$, where $\mathbf{v}_i$ is the velocity of the ith monomer. For a polymer at equilibrium the average $\langle \mathbf{v}_{\rm cm}\rangle = 0$. However, the typical or the rms velocity is

$$v_{\rm cm} = \sqrt{\frac{1}{N^2}\sum_{i,j=1}^{N}\langle \mathbf{v}_i\cdot\mathbf{v}_j\rangle} = \frac{v_{\rm th}}{\sqrt{N}}, \tag{4}$$

where $v_{\rm th} = \sqrt{d/\beta m}$ is the rms thermal velocity of a single monomer, while m is the mass of the monomer, and d is the spatial dimension. [In further (approximate) calculations we will omit d.] The time t it would take the polymer to move a distance equal to its own size $R = aN^\nu$ would be

$$t = R/v_{\rm cm} \approx a\sqrt{\beta m}N^{\nu+1/2}. \tag{5}$$

We expect that this will also be the time scale of the slowest internal motion of the polymer. It is natural to define a "slow motion" velocity v, such that during the time t the polymer is not dragged more than R, i.e., we must require $v < v_{\rm cm}$. In other words, for the ND the borderline critical velocity v_c coincides with the typical velocity of the center of mass $v_{\rm cm}$, or

$$v_c \approx \frac{1}{\sqrt{\beta m}}N^{-1/2}. \tag{6}$$

The ND approach neglects the interactions of a polymer with the surrounding fluid and therefore its practical usefulness is limited. However, it presents a theoretically important case that formed an essential part of the original proof of JE [18,19], and provides important insights into the relations between the "regular" mechanics and the thermal physics. It also can be viewed as a limiting case of a general Langevin equation.

Alternatively, we can consider motion of the polymer in a very viscous fluid, where the inertia can be neglected on sufficiently long time scales. In this example we neglect hydrodynamic interactions, i.e., we consider the "free-draining" [28] regime. Such motion can be described by the *overdamped Langevin dynamics* (OLD). In the overdamped regime, the center of mass of an N-monomer polymer in free space performs diffusion characterized by a diffusion constant D, which is N times smaller than the diffusion constant D_0 of a single monomer. Therefore, the time t it takes it to diffuse a distance $R = aN^\nu$ is

$$t \approx \frac{R^2}{D} = \frac{a^2 N^{2\nu}}{D_0/N} = \frac{a^2}{D_0} N^{2\nu+1}. \tag{7}$$

This is also the slowest relaxation time of an internal mode of the polymer [4,28].

If the polymer is being dragged with a velocity v, we would consider such motion "slow" if during the same time t, the distance vt that the polymer is dragged does not exceed R. This means that we need to have $v < \frac{D_0}{a} N^{-1-\nu}$, or

$$v_c \approx \frac{D_0}{a} N^{-1-\nu}. \tag{8}$$

When hydrodynamic interactions are important (the Zimm regime [4,29]), a long polymer is not "transparent" to the surrounding liquid, and can be treated as a sphere of radius R diffusing in a liquid of viscosity η [4] with a diffusion constant $D \approx 1/\beta\eta R$, where we omitted a dimensionless prefactor. The time it takes for such a polymer to diffuse a distance R is $t \approx R^2/D \approx \beta\eta R^3$, which leads to

$$v_c \approx \frac{k_B T}{\eta R^2} \approx \frac{k_B T}{\eta a^2} N^{-2\nu}. \tag{9}$$

The arguments presented in this section are equally valid for a polymer in free space or near a repulsive wall, because in both cases the polymer will have similar relaxation times.

III. GAUSSIAN POLYMER IN FREE SPACE

The arguments presented in the previous section were valid for a broad class of polymer types and interactions between monomers. In this section we consider a simple model of an ideal polymer, in which we neglect the interactions between nonadjacent monomers of the chain, that are usually important in good solvents. The model only retains the linear connectivity of the monomers and is analytically solvable. Ideal polymers rarely represent experimental systems, but the scaling properties of their static and dynamic characteristics provide guidance to the treatment of more realistic and complicated models [4].

Consider a linear chain of N identical monomers of mass m connected by springs with constants k, such that the potential energy is given by $\frac{1}{2}k\sum_{i=1}^{N}(x_i - x_{i-1})^2$, where x_i ($i = 1,\dots,N$) are the positions of the monomers, while x_0 is the position of the end point to which the first monomer is connected, as depicted in Fig. 2. Such an energy describes the Gaussian model of an ideal polymer, which in the polymer literature is well known as Rouse model [28], although the latter term is also used to describe the type of dynamics, rather than the polymer structure. (The term "Gaussian" refers to the functional shape of the Boltzmann weight of this energy.) The microscopic length a is given by the rms separation between

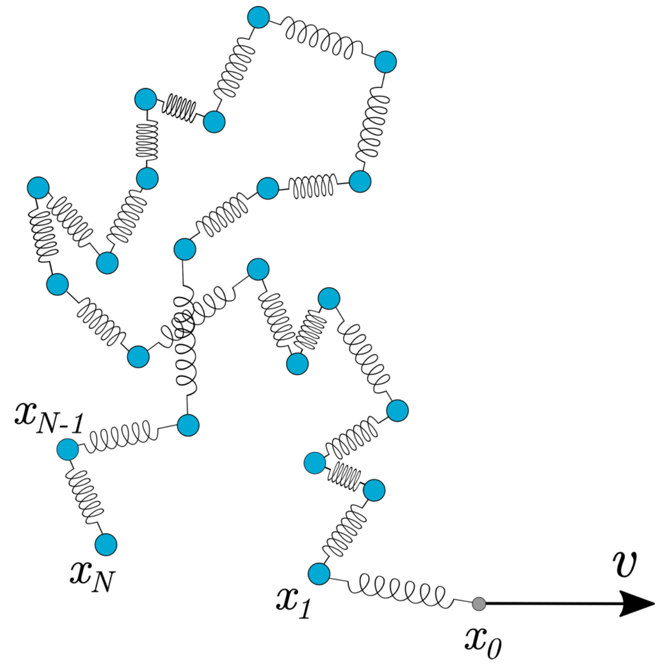

FIG. 2. A beads-and-springs model of a Gaussian (Rouse) chain is being dragged in free space by pulling its end point x_0 with a constant velocity v, such that $x_0 = vt$. Note, that we consider only a one-dimensional dynamical problem, and the second dimension in this figure is for illustration purpose only.

two consecutive monomers, i.e., $a^2 \equiv \langle (x_i - x_{i-1})^2 \rangle = 1/\beta k$. We can consider motion in three-dimensional space, with monomers positioned at $\mathbf{r}_i$. However, the particular form of the potential $\frac{1}{2}k(\mathbf{r}_i - \mathbf{r}_{i-1})^2$ splits into three independent parts and the motions in different space directions are independent. Thus, the only nontrivial part of the problem is in the direction parallel to the velocity with which the point at $\mathbf{r}_0$ is being dragged. This reduces the problem to a single space dimension.

The problem of *stretching* a Gaussian chain, when ΔF increases as a result of the external work, has already been solved for OLD, and the distribution of work has been calculated analytically [30,31]. We apply the same technique to a problem with slightly different boundary conditions, for both ND and OLD cases, and have a different goal: We consider the particular case of dragging the polymer in free space, where the free energy difference ΔF between the equilibrated final and initial states vanishes. In this section we find analytical expressions for $P(W)$, as well as v_c. The ND and OLD cases can be viewed as two extremes of the general Langevin equation for the system.

A. Analytical calculation of $P(W)$

In the absence of friction and thermal noise, the equation of motion of the nth monomer ($1 \leqslant n \leqslant N-1$) is governed by the ND equations

$$\ddot{x}_n = -\omega^2(2x_n - x_{n+1} - x_{n-1}), \tag{10}$$

and for $n = N$

$$\ddot{x}_N = -\omega^2(x_N - x_{N-1}), \tag{11}$$

where $\omega \equiv \sqrt{k/m}$. It is more convenient to work in a reference frame which moves with x_0, i.e., with a constant velocity v such that the position of the nth monomer (in the moving system) is $\tilde{x}_n = x_n - vt$. In this reference frame the equations of motion can be separated into N independent (Rouse [28]) eigenmodes by decomposing the position of the nth monomer into its discrete Fourier components,

$$\tilde{x}_n = A \sum_{q=1}^{N} \tilde{x}_q \sin(\alpha_q n), \tag{12}$$

where $\tilde{x}_q$ is the amplitude of the qth mode, and $A = \sqrt{\frac{2}{N+\frac{1}{2}}}$, while $\alpha_q = \frac{\pi(q-\frac{1}{2})}{N+\frac{1}{2}}$ was chosen to satisfy the boundary conditions, where one end of the polymer is fixed ($\tilde{x}_0 = 0$) and the other end ($\tilde{x}_N$) is free. The equations of motion remain the same in the moving system, with x replaced by $\tilde{x}$. Substituting Eq. (12) into Eq. (10) produces the equation of motion for the qth eigenmode in the moving reference frame,

$$\ddot{\tilde{x}}_q = -4\omega^2 \sin^2(\alpha_q/2)\tilde{x}_q, \tag{13}$$

which is a simple harmonic oscillator with frequency ω_q defined by

$$\omega_q^2 \equiv 4\omega^2 \sin^2(\alpha_q/2). \tag{14}$$

The *constant* pulling velocity can be represented (for any $n = 1, \ldots, N$) as

$$v = A \sum_{q=1}^{N} v_q \sin(\alpha_q n). \tag{15}$$

In this particular case of constant pulling velocity, v_q can be simply expressed via the inverse transform as $v_q = A\sum_{n=1}^{N} v \sin(\alpha_q n) = \frac{1}{2}Av\cot(\alpha_q/2)$ and used to transform the solution back to the laboratory frame,

$$x_n = \tilde{x}_n + vt \tag{16}$$

$$= A \sum_{q=1}^{N} \tilde{x}_q \sin(\alpha_q n) + A \sum_{q=1}^{N} v_q \sin(\alpha_q n)t \tag{17}$$

$$= A \sum_{q=1}^{N} \underbrace{(\tilde{x}_q + v_q t)}_{x_q} \sin(\alpha_q n). \tag{18}$$

Here, we defined $x_q = \tilde{x}_q + v_q t$, and the equation for the qth eigenmode in the laboratory frame is given by

$$\ddot{x}_q = -\omega_q^2 (x_q - v_q t). \tag{19}$$

This can be viewed as N independent simple harmonic oscillators with frequencies ω_q, being pulled by effective velocities v_q. Note that, for large N, the frequency of the lowest mode $\omega_{q=1} \sim \omega N^{-1}$ corresponds to the time it would take the polymer to move a distance R, as in Eq. (5) with $\nu = 1/2$.

We now examine the other extreme of this problem, in which the polymer is moving in a very viscous fluid, so that the inertia term can be neglected, and its motion is described by OLD. The equation of motion of the nth monomer, for $1 \leqslant n \leqslant N-1$, is given by

$$\gamma \dot{x}_n = -k(2x_n - x_{n+1} - x_{n-1}) + \eta_n(t), \tag{20}$$

and for $n = N$

$$\gamma \dot{x}_N = -k(x_N - x_{N-1}) + \eta_N(t), \tag{21}$$

where γ is the friction coefficient and $\eta_n(t)$ is the thermal noise associated with the nth monomer. The thermal noise is chosen to be white Gaussian noise which satisfies $\langle \eta_n(t) \rangle = 0$ and $\langle \eta_n(t)\eta_{n'}(t') \rangle = 2\gamma k_B T \delta(t-t')\delta_{nn'}$. The same decomposition that was applied to the position x_n and the pulling velocity v in the ND case, can be applied in this case too, while the decomposition of the noise is

$$\eta_n(t) = A \sum_{q=1}^{N} \eta_q(t) \sin(\alpha_q n), \tag{22}$$

where $\eta_q(t)$ is the effective thermal noise acting on the qth eigenmode, which satisfies $\langle \eta_q(t) \rangle = 0$ and $\langle \eta_q(t)\eta_{q'}(t') \rangle = 2\gamma k_B T \delta(t-t')\delta_{qq'}$.

Similarly to the ND case, the system is decomposed into N independent (Rouse) eigenmodes, where each one represents an independent overdamped harmonic oscillator that is being dragged with an effective velocity v_q. Each eigenmode satisfies

$$\dot{x}_q = -\frac{1}{\tau_q}(x_q - v_q t) + \frac{1}{\gamma}\eta_q, \tag{23}$$

where

$$\tau_q \equiv \frac{\tau}{4\sin^2 \alpha_q/2} \tag{24}$$

is the relaxation time of the qth eigenmode, and $\tau \equiv \gamma/k$. As we can see, the largest relaxation time $\tau_{q=1} \sim \tau N^2$ (for large N) coincides with the time it takes the center of mass of the polymer to diffuse a distance R [Eq. (7)]. During the time τ a monomer moves an approximate distance $a \approx \sqrt{D_0 \tau}$, where $D_0 = k_B T/\gamma$.

Both in the ND and OLD cases we can treat the system as N independent harmonic oscillators, and write the total work W done on the system (by an external agent) during the pulling, as a sum of works W_q done on each single effective oscillator, i.e.,

$$W = \sum_{q=1}^{N} W_q. \tag{25}$$

Each W_q has a Gaussian distribution with mean μ_q and variance σ_q^2, such that $\mu_q = \frac{\beta}{2}\sigma_q^2 = 2mv_q^2 \sin^2(\omega_q t/2)$ for the ND case, and $\mu_q = \frac{\beta}{2}\sigma_q^2 = \gamma\tau_q v_q^2(e^{-t/\tau_q} + t/\tau_q - 1)$ for the OLD case (as shown in the Appendix). Therefore, W also has a Gaussian distribution characterized by mean $\mu = \sum_{q=1}^{N} \mu_q$ and variance $\sigma^2 = \sum_{q=1}^{N} \sigma_q^2$.

In the ND case the mean work is

$$\mu_{\rm ND}(t) = \frac{\beta}{2}\sigma_{\rm ND}^2(t) = \sum_{q=1}^{N} 2mv_q^2 \sin^2\left(\frac{\omega_q t}{2}\right). \tag{26}$$

For small q the frequencies ω_q have almost integer ratios with $\omega_{q=1}$ and, not surprisingly, $\mu_{\rm ND}(t)$ is "almost" a periodic function. For $N \gg 1$, it looks as a triangular wave depicted

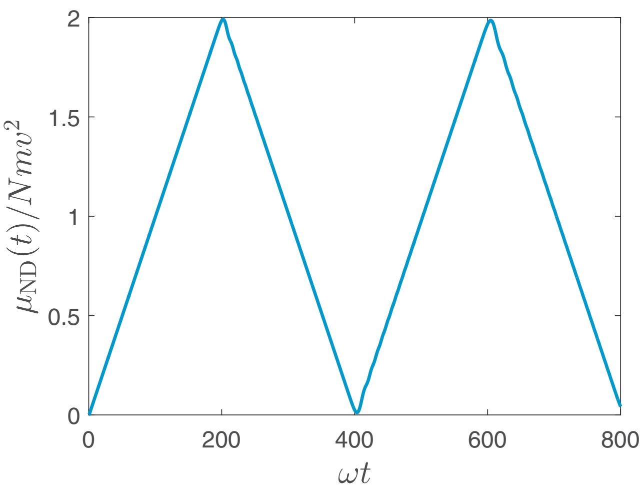

FIG. 3. Normalized mean work $\mu_{\rm ND}$ for $N = 100$ as a function of time t (see text). For large N, $\mu_{\rm ND}$ resembles a triangular wave with a period $T = 4N/\omega$. (For large t the apparent periodicity disappears.)

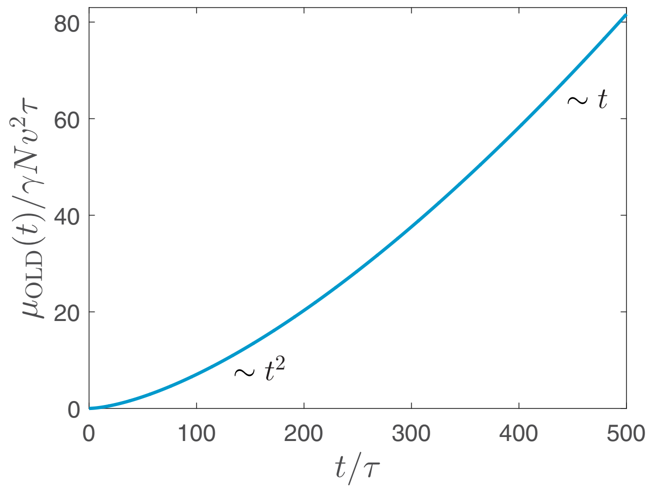

FIG. 4. Normalized mean work $\mu_{\rm OLD}$ as function of time t for $N = 100$ (see text). At short times, $\mu_{\rm OLD}$ is parabolic, and for large times it grows linearly with t.

in Fig. 3 of amplitude $2Nmv^2$ with period $T = 2\pi/\omega_{q=1} \approx 4N/\omega$. However, higher frequencies have more complicated dependence on q [see Eq. (14)], and after many oscillations the appearance of the periodicity vanishes.

It is interesting to note that in terms of dimensionless variable $y \equiv \beta W$, the probability distribution of the work W has a very simple form,

$$\tilde{P}(y) = \frac{1}{\sqrt{4\pi\tilde{\mu}}} \exp\left[-\frac{(y-\tilde{\mu})^2}{4\tilde{\mu}}\right], \tag{27}$$

where we used the relation (26) between the mean and the variance and the reduced mean $\tilde{\mu} \equiv \beta\mu_{\rm ND}$. For large N and moderate times it is convenient to express $\tilde{\mu}$ via triangular wave function S (as in Fig. 3) of unit amplitude and period leading to $\tilde{\mu} = 2\beta N m v^2 S(t/T)$. If we measure the pulling velocity in units of v_c [as defined in Eq. (6)], i.e., $u \equiv v/v_c$, and the total pulling length L in units of polymer size R, $\ell \equiv L/R$, then the expression for the reduced mean further simplifies to

$$\tilde{\mu} = 2u^2 S(\ell/4u), \tag{28}$$

where we used the fact that $R = aN^{1/2}$ and the mean separation between the monomers is $a = 1/\omega\sqrt{\beta m}$.

In the OLD case the mean work is

$$\mu_{\rm OLD}(t) = \frac{\beta}{2}\sigma^2_{\rm OLD}(t) = \sum_{q=1}^{N} \gamma\tau_q v_q^2\left(e^{-t/\tau_q} + \frac{t}{\tau_q} - 1\right), \tag{29}$$

which is depicted in Fig. 4. For short times ($t \ll \tau_{q=N} \approx \tau$), it increases parabolically with time: $\mu_{\rm OLD}(t) \approx \frac{1}{2}\frac{\gamma}{\tau}v^2t^2 = \frac{1}{2}k(vt)^2$. This corresponds to an external force stretching a single spring of the first monomer connected to x_0, since during time $t < \tau$ only x_0 moves, and the rest of the system "does not know" yet that it is being pulled. In the long time regime ($t \gg \tau_{q=1} \approx \tau N^2$) the mean work grows linearly with time as $\mu_{\rm OLD}(t) \approx \gamma N v^2 t$. This represents the work against friction performed by dragging N monomers together. (Other eigenmodes are already relaxed in the system.)

B. Analysis of the results

The JE in Eq. (3) can be cast in the form of a cumulant expansion [18,32]:

$$\Delta F = -\frac{1}{\beta}\ln\langle e^{-\beta W}\rangle = \mu - \frac{\beta}{2}\sigma^2 + \cdots. \tag{30}$$

If $P(W)$ is a Gaussian, as in the case of our model in free space, this expansion terminates at the second term. In addition, in free space displacement of the polymer does not modify its free energy, i.e., $\Delta F = 0$. From Eq. (30) we conclude that in free space $\mu = \frac{\beta}{2}\sigma^2$, which coincides with the analytical results obtained by a direct calculation in the previous subsection. In the particular case of Gaussian $P(W)$, $G(W) \equiv e^{-\beta W}P(W)$ is another Gaussian shifted by 2μ towards lower values of W. For slow motion we must have $\mu < \sigma$, i.e., the mean work (and the shift between P and G) does not exceed the width of the distribution. At the critical velocity this relation becomes an equality. Due to the relation between μ and σ, this condition becomes

$$\mu \approx 2k_{\rm B}T. \tag{31}$$

In the case of ND, the mean value of work is bounded by $2Nmv^2$, and therefore, from Eq. (31) we find that $v_c \approx N^{-1/2}/\sqrt{\beta m}$, which is exactly v_c that we found in Eq. (6).

In the OLD case, $\mu_{\rm OLD}$ increases monotonically with time, making the free energy reconstruction more difficult as t grows. We would like to drag the polymer a distance at least equal to its size, i.e., $L = vt \sim a\sqrt{N}$. (In free space it is a somewhat arbitrary choice, but in the next section we will consider a polymer being dragged away from a wall, and then such a choice of distance becomes crucial.) For such L the condition in Eq. (31) translates into $a\gamma N^{3/2}v_c \approx k_{\rm B}T$, which defines the critical velocity,

$$v_c \approx \frac{1}{a\gamma\beta}N^{-3/2}. \tag{32}$$

Substituting $a \approx \sqrt{D_0\tau}$ brings us back to the same critical velocity that was found in Eq. (8), with $\nu = 1/2$. In terms of dimensionless variable $y = \beta W$ the probability distribution of work is given by Eq. (27), with reduced mean $\tilde{\mu} \equiv \beta\mu_{\rm OLD}$. For times larger than the relaxation time of the polymer and for $N \gg 1$, we get $\tilde{\mu} = \beta\gamma N v^2 t$, which can be conveniently expressed via relative distance $\ell = L/R$ and relative velocity $u = v/v_c$, where v_c was derived in Eq. (32), leading to

$$\tilde{\mu} = u\ell. \tag{33}$$

We note that both in ND and OLD cases for large N the work distribution is described by Eqs. (27), (28), and (33), which for fixed dimensionless u and ℓ are independent of N. This is a direct consequence of the scaling of internal relaxation times and internal length scales related to scale-invariant internal structures of the polymer [4], when only the polymer size R and the largest relaxation time determine the time and length scales of the internal modes.

Hydrodynamic interactions cannot be accurately treated even for ideal polymers, since the equations of motion do not split into a set of independent equations for each q mode, as in Eq. (23). However, it has been shown [29] that close to equilibrium such interactions can be *mimicked* by replacing fixed γ by a power law of q in the Fourier space, i.e., modifying τ_q in Eq. (24) by an extra power of q. [This change also requires a proper change in the noise correlation $\langle\eta_q(t)\eta_{q'}(t')\rangle$.] While we expect these changes to correctly reproduce the near-equilibrium behavior of the system, as well as the value of v_c in Eq. (9), we do not expect them to produce a good approximation for $P(W)$ for $v \gg v_c$.

IV. POLYMER NEAR A WALL

In this section we consider the Gaussian (Rouse) chain dragged away from a repulsive wall. At time $t = 0$ the polymer is in equilibrium near the wall at $x_0 = 0$, and is being dragged away from the wall at a constant velocity v, i.e., $x_0 = vt$, as illustrated in Fig. 5. If the final distance L of the polymer from the wall is significantly larger than R, then in the final equilibrated state the free energy will be equal to its value in free space, and in accordance with Eq. (2) $\Delta F = -\frac{1}{2}k_BT\ln N$. Unlike the simple case considered in the previous section, we can no longer expect a simple relation between μ and σ, and $P(W)$ will not have a Gaussian form.

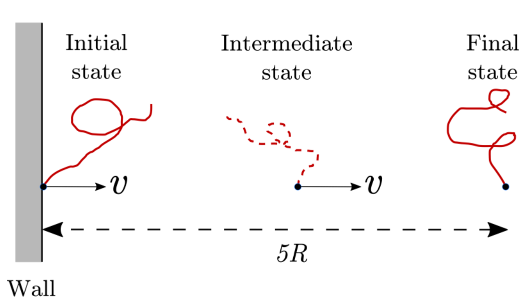

FIG. 5. At $t = 0$ a polymer is at equilibrium with one of its ends attached to the wall. At $t > 0$ it is dragged away from the wall with a constant velocity v until it reaches a distance $L = 5R$, where it is equilibrated. We consider a one-dimensional problem, and the transverse dimension is only for illustration purposes.

Our results rely on a numerical solution of Newton's equations in the ND case, and on a solution of an overdamped Langevin equation in the OLD case [33,34]. In both cases the calculation begins by choosing a properly weighted initial configuration. The coordinates of the monomers are then advanced in time until x_0 reaches the value $L = 5R$. Integration of the external force that needs to be applied to x_0 to keep it moving at a constant velocity v produces the work W of the external agent. Each calculation was repeated $\mathcal{N} = 10^3$ times. Every time a new initial equilibrium state was selected, and, in the OLD case a new thermal noise function was generated. Such calculations produce a numerical estimate of $P(W)$ and can be used to produce a numerical estimate of ΔF. We repeated the calculations for chain sizes N ranging from 10 to 100, and for each chain size repeated the calculation for dragging velocities ranging from $0.1v_c$ to $5v_c$. In this section we present a partial set of our results.

Since the exactly known ΔF is proportional to $-\ln N$, the graphs of $P(W)$ shift towards more negative values of W with increasing N. For an easy comparison of the results with different chain sizes, it is convenient to present all the functions in terms of the dissipated work $W_{\rm d} = W - \Delta F$, rather than the entire work W. Furthermore, we will use the dimensionless variable $y \equiv \beta W_d$. The probability density $\tilde{P}(y)$ is simply related to $P(W)$ by $\tilde{P}(y) = P(W_{\rm d} + \Delta F)/\beta$. Similarly, a new shifted function $\tilde{G}(y) \equiv e^{-y}\tilde{P}(y)$ can be used. In this notation the probability density is normalized, i.e., $\int_{-\infty}^{\infty}\tilde{P}(y)dy = 1$ and the relation (3) has the simple form $\int_{-\infty}^{\infty}\tilde{G}(y)dy = 1$. While these two integrals impose some restrictions on the shape of $\tilde{P}$, there is still plenty of room for dependence of this function on N or v and on the type of dynamics (ND or OLD). Normally the term "dissipation" implies positive W_d or $y > 0$. In macroscopic systems for the average $W_{\rm d}$ this is referred to as the Clausius inequality. However, a particular experiment may violate this inequality [24]. This is very unlikely, and it can be shown that the probability of $y < -\zeta$ (for $\zeta > 0$) is bounded by $e^{-\zeta}$ [24]. This means that $W_{\rm d}$ can be only a few times $-k_BT$, independently of the system size. This inequality further restricts the possible shapes of $\tilde{P}$.

The solid lines in Figs. 6 and 7 depict the the probability distributions of the dissipated work $W_{\rm d}$ for short polymers ($N = 10$), for the ND and OLD cases, respectively. These histograms are results of $\mathcal{N} = 10^3$ repeated numerical experiments. The size of the bin was selected for convenient presentation of the results. (Calculation of ΔF from the data is performed directly from the set of measured $W_{\rm d}$s rather than from these histograms.) All distributions have a tail in the negative y region but most of such "Clausius-inequality-violating" events are within one unit away from 0. For small velocities $v = 0.1v_c$ [graphs (a)] the distributions represent a process that is rather close to quasistatic, i.e., they are narrow and close to 0, and the mean dissipation satisfies $\langle y\rangle = \beta\langle W_{\rm d}\rangle \ll 1$. When the polymer is dragged away at a large velocity $v = 2v_c$ [graphs (b)] the distributions are shifted towards larger y values, corresponding to an external agent pulling the polymer away from the wall, in contrast with the low-velocity case when the force is mostly towards the wall to maintain a constant velocity. The area under the solid lines in all the graphs is 1 due to normalization.

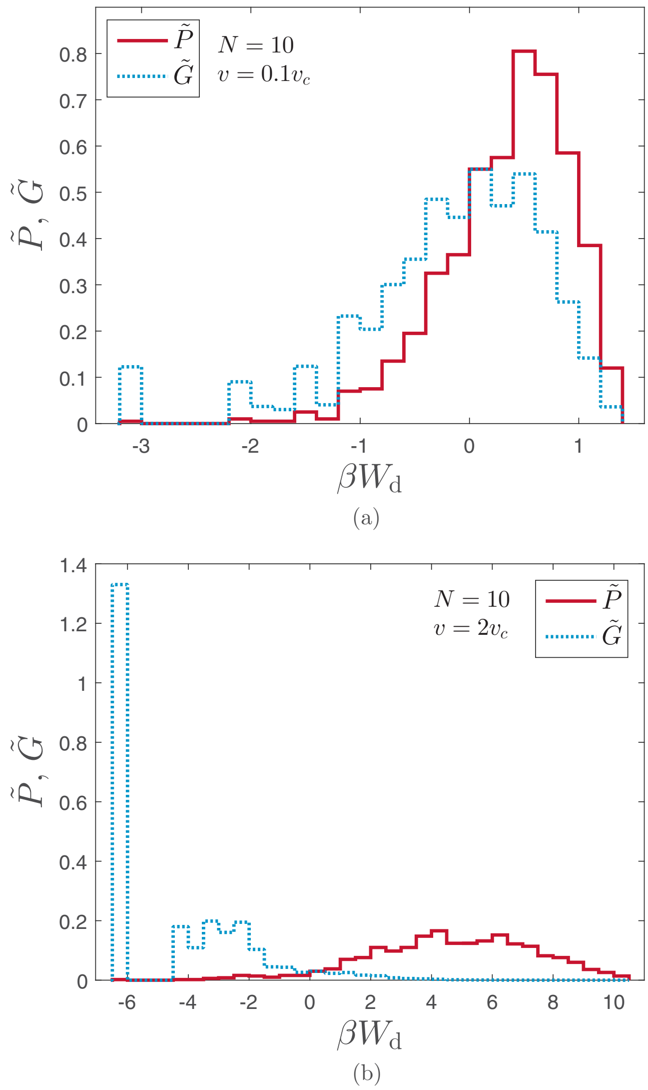

FIG. 6. Results for the dissipated work distribution in the ND case extracted from a sample of $\mathcal{N} = 10^3$ repeated calculations for a short polymer ($N = 10$) dragged away from a repulsive wall. The solid line histograms depict the numerically calculated probability density $\tilde{P}(y)$ measured as a function of $y = \beta W_{\mathrm{d}}$, where W_{d} is the dissipated work. Dotted lines represent the shifted function $\tilde{G}(y) = e^{-y}\tilde{P}(y)$. The polymer was dragged at a constant velocity (a) $v = 0.1v_c$ and (b) $v = 2v_c$.

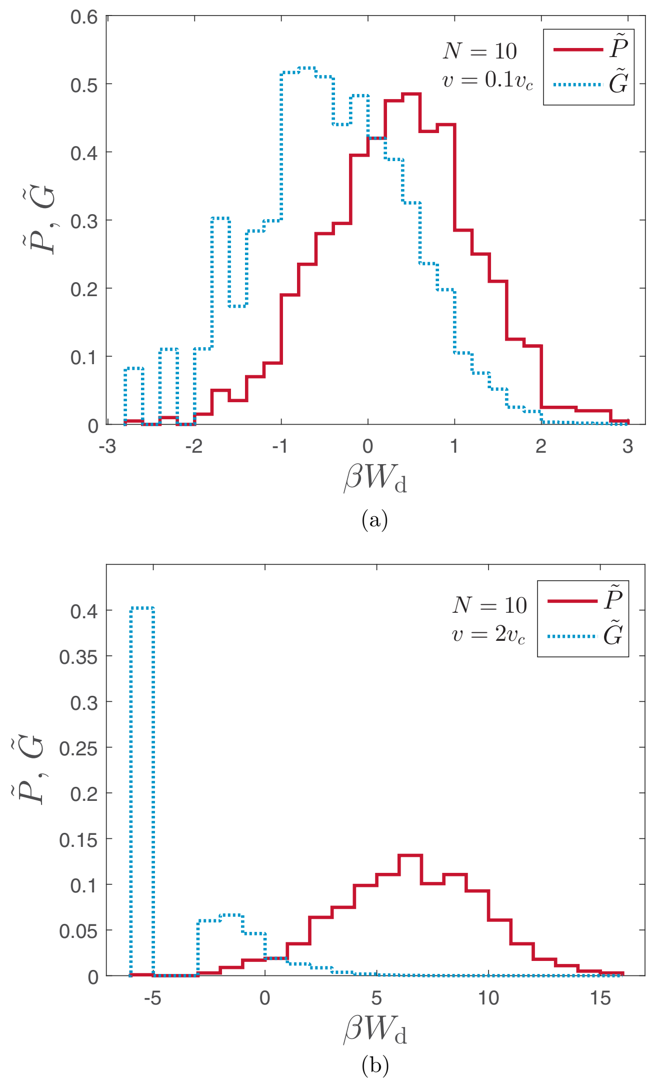

FIG. 7. Results for the dissipated work distribution in the OLD case. All the notations are the same as in Fig. 6.

The dotted histograms in Figs. 6 and 7 represent the shifted functions $\tilde{G}$, and they were constructed from the values of the solid histograms by multiplying them by e^{-y}. To correctly reproduce the known value of ΔF, the area under $\tilde{G}$ must be 1. This indeed happens in the low-velocity graphs (a), where the area does not deviate from 1 by more that 0.1 even for a moderate number $\mathcal{N}$ of experiments. At high velocities [graphs (b)] the reconstructed $\tilde{G}$ is significantly shifted compared to $\tilde{P}$, and is reconstructed from the poor quality tail of $\tilde{P}$. For $y < -1$ most bins correspond either to 0 or to 1 event found in that range, which explains the noisy behavior of $\tilde{G}$. The area under the $\tilde{G}$ curve at high velocities significantly deviates from 1. This means that the reconstructed free energy difference will have significant errors. We used our data sets to directly evaluate the free energy difference from the expression

$$\Delta F_{\mathrm{num}} = -\frac{1}{\beta}\ln\left(\frac{1}{\mathcal{N}}\sum_{i=1}^{\mathcal{N}} e^{-\beta W_i}\right), \tag{34}$$

where W_i is the work associated with the ith repetition of the calculation. When these estimates of the free energy difference were compared with the exactly known ΔF, we saw (for N ranging from 10 to 100) a fast deterioration of accuracy when v exceeded v_c. This result confirms our expectation that v_c serves as a borderline velocity between "slow" and "fast" processes for all values of N in the problem of a polymer near a wall.

In the previous section we found analytically that the work distribution for a polymer of large N in free space is described by Eqs. (27), (28), and (33), which for fixed dimensionless u and ℓ are independent of N. We argued that in free space this is a direct consequence of the scaling of internal relaxation times and internal length scales [4]. Such a lack of N dependence is rather natural even in the presence of a wall, since the equations of motion can be reformulated in properly scaled variables in the $N \to \infty$ limit, indicating the existence of such a limit. In

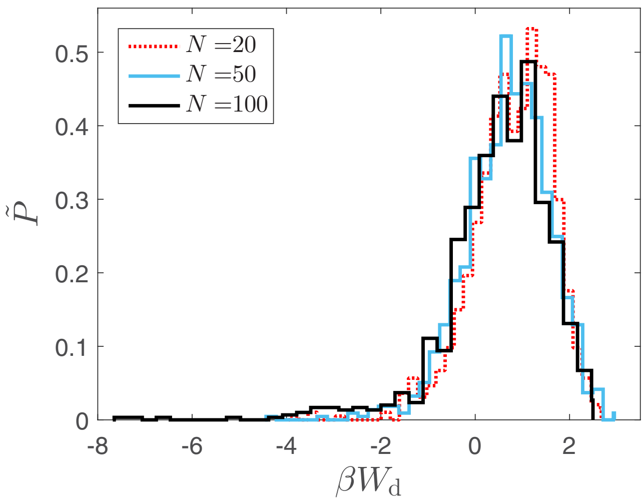

FIG. 8. Results for the dissipated work distribution in the ND case extracted from a sample of $\mathcal{N} = 10^3$ repeated calculations for polymers of three different Ns as indicated in the legend. Each calculation was performed with the same relative velocity $u = 1$, or $v = v_c$.

free space, $\Delta F = 0$, or $W_\mathrm{d} = W$. In the presence of the wall, a simple free space result is no longer possible, due to the N dependence of ΔF. Nevertheless, by considering W_d we eliminate the leading N dependence, and may hope to get an N-independent limit. Figure 8 depicts $\tilde{P}(y)$ in the ND case for several values of N, when each case has been calculated with the same *relative* velocity u. Since v_c decreases with increasing N, the velocity v was also decreased. We note that three different Ns produce rather similar graphs. A change of u produces *different* graphs, but again, they seem to be almost independent of N. In the third paragraph of this section we mentioned that there were several constraints on the shape of $\tilde{P}(y)$. Therefore, the similarity of the graphs is not surprising. Nevertheless it is possible that in these scaled variables there is an $N \to \infty$ limit of this graph which our numerical graphs are approaching. We could see this property explicitly in the solution of a polymer in free space. Due to scaling of the dynamical properties of a polymer, it is possible that similar features exist in the more complicated case of a polymer near a wall. Similar behavior is also observed in the OLD case, although the graphs for the same u values differ slightly from the ND shapes discussed above.

V. DISCUSSION

We studied the problem of a flexible polymer being dragged with a constant velocity both in free space and in the vicinity of the wall, and argued that there exists a critical N-dependent pulling velocity v_c that separates the region of "easy" reconstruction of ΔF by means of the Jarzynski equality from the region of "impossible" reconstruction. The existence of a maximal deviation from equilibrium for which the reconstruction of ΔF is possible is well known from previous studies [20–23]. In the context of unfolding of a large molecule this was typically viewed as an event of a "single particle" escaping from one well into another [35], or a sequence of such events [13]. We attempted to integrate the well-known static and dynamic scaling properties of polymers into the description of their nonequilibrium motion. Our heuristic argument in Sec. II produced in the ND case the result $v_c \sim N^{-1/2}$ which was independent of the polymer type, while for OLD the result depended on the exponent ν. The numerical support of our claim is limited to the two simple cases of free space and repulsive wall for ideal polymers. We observed the lack of N dependence of the dissipated work distribution, but the range of Ns was rather limited, and much longer polymers need to be studied.

While our calculations were limited to the ideal polymers, some of the concepts can be generalized to more realistic models, such as the polymers in good solvents, when the interactions between nonadjacent monomers are important. In the latter case, the Rouse modes, such as $\tilde{x}_q$ in Eq. (12), are no longer the exact eigenmodes of the system. Nevertheless, the properly modified concept of Rouse modes is used to describe dynamics of the polymers [28]. We expect that this and other generalized concepts can be used to produce results described in Sec. II. Confirmation of this expectation will require detailed numerical simulations.

While the "free draining" regime provides an adequate description of the motion of polymers of moderate length, in experiments with longer polymers the hydrodynamic interactions play an important role. We briefly mentioned this regime in Sec. II. In accordance with Eq. (9) the typical critical velocity of a 1-μm size polymer will be slightly above 1 μm/s, which is one order of magnitude larger than the typical speeds in many experiments (see, e.g., [20]). The use of a constant dragging velocity significantly simplified our derivations. By contrast, in real experiments the force, rather than the speed, is controlled. However, in homogeneous polymers these two should exhibit a similar behavior.

ACKNOWLEDGMENTS

We thank Y. Hammer and M. Kardar for numerous discussions. We also thank them and D. J. Bergman for valuable comments about the manuscript. This work was supported by Israel Science Foundation Grant No. 453/17.

APPENDIX: DRAGGED HARMONIC OSCILLATOR

Our analytical treatment of the Gaussian polymer in free space relies on a decomposition into Rouse modes that are treated as simple dragged harmonic oscillators. The harmonic oscillator (HO) was one of the first systems used to demonstrate the workings of the JE [36]. The theoretical treatment of a dragged HO [37] followed an experimental study of the translation of a particle in a harmonic optical trap [38], which was designed to test violations of the second law of thermodynamics with findings consistent with a fluctuation theorem of Evans *et al.* [39].

Consider the motion of a particle of mass m at position x attached by a spring with force constant k to a point x_0, which moves with velocity v, i.e., at time t its position is $x_0 = vt$. In the ND case the equation of motion is

$$m\ddot{x} = -k(x - vt), \tag{A1}$$

and its solution is given by

$$x(t) = x^0 \cos(\omega t) + \left(\frac{p^0}{m\omega} - \frac{v}{\omega}\right)\sin(\omega t) + vt, \tag{A2}$$

where $\omega = \sqrt{k/m}$, and x^0, p^0 are the initial position and momentum of the particle, respectively, which are selected from a Gaussian distribution corresponding to the temperature of the system. For the OLD case the equation of motion is

$$\gamma \dot{x} = -k(x - vt) + \eta(t), \tag{A3}$$

where γ is the friction constant and random function $\eta(t)$ represents white Gaussian noise which satisfies $\langle \eta(t) \rangle = 0$ and $\langle \eta(t)\eta(t')\rangle = 2\gamma k_{\mathrm{B}} T \delta(t - t')$. The solution for this equation is given by

$$x(t) = x^0 e^{-t/\tau} + vt + \int_0^t \left(\frac{1}{\gamma}\eta(t') - v\right) e^{-(t-t')/\tau} dt', \tag{A4}$$

where $\tau = \gamma/k$ is the relaxation time of the oscillator. Note that both in ND and in OLD cases the position $x(t)$ has a Gaussian distribution since it is a linear combination of Gaussian variables. The work done on the oscillator during the dragging of x_0 at a constant velocity v is

$$W = -v \int_0^t k[x(t') - vt']dt'. \tag{A5}$$

Since $x(t)$ is known as function of the initial conditions and the realization of noise $\eta(t)$ (in the OLD case), the distribution $P(W)$ can be easily determined. Since $x(t)$ has a Gaussian distribution, the distribution of work $P(W)$ is also a Gaussian characterized by its mean $\mu = \langle W \rangle$ and variance $\sigma^2 = \langle W^2 \rangle - \langle W \rangle^2$.

Direct calculation of μ and σ, both in the ND and in the OLD cases, finds that these quantities are simply related: $\mu(t) = \frac{\beta}{2}\sigma^2(t)$. [This can also be viewed as a consequence of the JE for a Gaussian work distribution in a situation where the equilibrium free energy of an oscillator is independent of its position, as explained in the paragraph following Eq. (30).] In the ND case

$$\mu(t) = 2mv^2 \sin^2\left(\frac{\omega t}{2}\right). \tag{A6}$$

This $\mu(t)$ is periodic and vanishes after each complete period of the oscillator. In the OLD case

$$\mu(t) = \gamma \tau v^2 \left(e^{-t/\tau} + \frac{t}{\tau} - 1\right). \tag{A7}$$

This $\mu(t)$ increases monotonically with time. At large times the mean work is linear in t representing the work against friction.

[1] K. Binder, in *Phase Transitions and Critical Phenomena*, edited by C. Domb and J. L. Lebowitz (Academic Press, London, 1983), Vol. 8, pp. 1–144.
[2] K. De'Bell and T. Lookman, Rev. Mod. Phys. **65**, 87 (1993).
[3] E. Eisenriegler, *Polymers Near Surfaces: Conformation Properties and Relation to Critical Phenomena* (World Scientific, Singapore, 1993).
[4] P. G. de Gennes, *Scaling Concepts in Polymer Physics* (Cornell University Press, Ithaca, NY, 1979).
[5] J. L. Cardy and S. Redner, J. Phys. A **17**, L933 (1984).
[6] A. Grosberg, A. Khokhlov, and Y. Atanov, *Statistical Physics of Macromolecules* (AIP, New York, 1994).
[7] M. Rubinstein and R. Colby, *Polymer Physics* (Oxford University Press, New York, 2003).
[8] J. Zlatanova and K. van Holde, Mol. Cell **24**, 317 (2006).
[9] S. Leuba and J. Zlatanova, *Biology at the Single Molecule Level* (Pergamon Press, New York, 2001).
[10] G. Binnig, C. F. Quate, and C. Gerber, Phys. Rev. Lett. **56**, 930 (1986).
[11] S. Morita, R. Wiesendanger, and E. Meyer, *Noncontact Atomic Force Microscopy* (Springer, New York, 2002), Vol. 1.
[12] D. Sarid, *Scanning Force Microscopy* (Oxford University Press, New York, 1994).
[13] C. Bustamante, S. B. Smith, J. Liphardt, and D. Smith, Curr. Opin. Struct. Biol. **10**, 279 (2000).
[14] M. F. Maghrebi, Y. Kantor, and M. Kardar, Europhys. Lett. **96**, 66002 (2011).
[15] M. F. Maghrebi, Y. Kantor, and M. Kardar, Phys. Rev. E **86**, 061801 (2012).
[16] N. Alfasi and Y. Kantor, Phys. Rev. E **91**, 042126 (2015).
[17] Y. Hammer and Y. Kantor, Phys. Rev. E **92**, 062602 (2015).
[18] C. Jarzynski, Phys. Rev. Lett. **78**, 2690 (1997).
[19] C. Jarzynski, Phys. Rev. E **56**, 5018 (1997).
[20] J. Liphardt, S. Dumont, S. B. Smith, I. Tinoco, Jr., and C. Bustamante, Science **296**, 1832 (2002).
[21] G. Hummer and A. Szabo, Acc. Chem. Res. **38**, 504 (2005).
[22] G. Hummer and A. Szabo, Proc. Natl. Acad. Sci. USA **98**, 3658 (2001).
[23] N. C. Harris, Y. Song, and C.-H. Kiang, Phys. Rev. Lett. **99**, 068101 (2007).
[24] C. Jarzynski, Annu. Rev. Condens. Matter Phys. **2**, 329 (2011).
[25] R. C. Lua and A. Y. Grosberg, J. Chem. Phys. B **109**, 6805 (2005).
[26] I. Bena, C. van den Broeck, and R. Kawai, Europhys. Lett. **71**, 879 (2005).
[27] C. Jarzynski, Phys. Rev. E **73**, 046105 (2006).
[28] M. Doi and S. Edwards, *The Theory of Polymer Dynamics* (Oxford University Press, New York, 1986).
[29] B. H. Zimm, J. Chem. Phys. **24**, 269 (1956).
[30] A. Dhar, Phys. Rev. E **71**, 036126 (2005).
[31] T. Speck and U. Seifert, Eur. Phys. J. B **43**, 521 (2005).
[32] G. Hummer, J. Chem. Phys. **114**, 7330 (2001).
[33] W. H. Press, S. A. Teukolsky, W. T. Vetterling, and B. P. Flannery, *Numerical Recipes in C*, 2nd ed. (Cambridge University Press, Cambridge, England, 1992).
[34] D. W. Heermann, *Computer Simulation Methods in Theoretical Physics* (Springer, Berlin, 1990).
[35] I. Junier, A. Mossa, M. Manosas, and F. Ritort, Phys. Rev. Lett. **102**, 070602 (2009).
[36] O. Mazonka and C. Jarzynski, arXiv:cond-mat/9912121.
[37] R. van Zon and E. G. D. Cohen, Phys. Rev. E **67**, 046102 (2003).
[38] G. M. Wang, E. M. Sevick, E. Mittag, D. J. Searles, and D. J. Evans, Phys. Rev. Lett. **89**, 050601 (2002).
[39] D. J. Evans, E. G. D. Cohen, and G. P. Morriss, Phys. Rev. Lett. **71**, 2401 (1993).